Rapid assessment of the fuel economy capability of parallel and series-parallel hybrid electric vehicles

Rapid assessment of the fuel economy capability of parallel and series-parallel hybrid electric vehicles

Pier Giuseppe Anselma,[a,b,c,*] Atriya Biswas,[c] Giovanni Belingardi,[a,b] Ali Emadi,[c]

[a]*Department of Mechanical and Aeropsace Engineering (DIMEAS), Politecnico di Torino, 10129 Torino, Italy*

[b]*Center for Automotive Research and Sustainable Mobility (CARS), Politecnico di Torino, 10129 Torino, Italy*

[c]*McMaster Institute for Automotive Research and Technology (MacAUTO), McMaster University, L8P 0A6 Hamilton (ON), Canada*

Highlights

- Optimal control of stepped gear transmission (SGT) hybrid electric vehicles (HEVs).
- Account for both fuel economy and drivability.
- A rapid near-optimal off-line control algorithm is developed.
- Comparable results with dynamic programming while cutting down computational cost.
- Ease of use in advanced design and calibration methodologies for SGT HEVs.

Abstract

Efficiently solving the off-line control problem represents a crucial step to predict the fuel economy capability of hybrid electric vehicles (HEVs). Optimal HEV control approaches implemented in literature usually prove to be either computationally inefficient or sub-optimal. Moreover, they often neglect drivability and comfort associated to the generated control actions over time. This paper therefore aims at introducing a rapid near-optimal approach to solve the off-line control problem for parallel and series-parallel HEV powertrains while accounting for drivability criteria such as the frequency of gear shifts and the number of activations of the thermal engine. The performance of the introduced slope-weighted energy-

* Corresponding author. e-mail: pier.anselma@polito.it

based rapid control analysis (SERCA) algorithm is compared with the global optimal benchmark provided by dynamic programming (DP) for both the parallel and the series-parallel HEV layouts over different driving missions. Results demonstrate how the SERCA algorithm can produce comparable control results with respect to DP by limiting the increase in the estimated fuel consumption within 2.2%. The corresponding computational time can be simultaneously reduced by around 99.5% while ensuring a limited number of gear shifts and engine activations over time. Engineers could therefore potentially implement the proposed SERCA algorithm in design and calibration procedures of parallel and series-parallel HEVs to accelerate the overall vehicle development process.

Keywords: fuel economy; hybrid electric vehicle (HEV); optimal energy management; parallel layout; rapid control

1. Introduction

Hybrid electric vehicles (HEVs) currently represent a profitable technology to potentially comply with worldwide tightening CO_2 emission regulations and simultaneously accomplishing customers' needs [1][2]. Moreover, HEVs constitute an important stage in the global paradigm shift of the transportation sector towards electrification [3]. HEVs generally embed an internal combustion engine (ICE) and one or more electric motor/generators (MGs). The presence of different power components aims at reducing the overall fuel consumption by increasing the flexibility in the HEV powertrain operation [4][5].

Different categories of HEV powertrain architectures can be defined according to the position of the power components and the type of transmission embedded [6]. At the most general level, HEVs can be classified into electrically variable transmission (eVT) type and stepped gear transmission (SGT) type. eVT HEVs are based on planetary gear sets, composed of a ring gear, a carrier and a sun gear. These two degrees of freedom mechanical devices enable decoupling the ICE rotational speed from the vehicle linear speed, thus enhancing the potential of fuel economy through higher flexibility of operation [7][8]. Nevertheless, these HEVs typically require two MGs (one for propelling the vehicle and one for generating electrical energy from the mechanical energy provided by the ICE) and therefore represent complex powertrain architectures [9]. Moreover, the mechanical coupling of planetary gear sets does not allow to direct the ICE mechanical energy entirely to the wheels, thus partially compromising the potential drivability of these vehicles. Finally, the increased number of gear engagement points in planetary gear devices intensifies the overall transmission meshing losses [10]. On the other hand, SGT HEVs preserve the typical structure of road vehicle drivetrains being equipped with the ICE, a clutch, a gearbox and final drive in series. One or multiple MGs can then be added to the drivetrain in specific positions according to the designers' choice. P0, P1, P2, P3 and P4 locations are particularly defined depending on the MG being located upstream the ICE (belt-driven), downstream the ICE (keyed directly onto the same shaft), between the ICE and the transmission gearbox (being linked through clutch connections), between the transmission gearbox and the final drive and separately from the ICE in the rear axle (that performs as pure electric driven axle) respectively [11]. The main disadvantage of SGT HEVs compared to eVT HEVs is represented by the speed of the ICE being dependent on the vehicle speed. However, in SGT HEV layouts both ICE and MGs can directly deliver tractive power to the driven wheel shaft, thus making these vehicles appealing from the points of view of drivability, towing capability and maximum achievable speed [12]. Moreover, relatively little changes are required to convert a conventional road vehicle drivetrain into a SGT HEV powertrain, thus enhancing the ease of production of these HEVs from car makers' perspective [13].

Advanced computer-aided engineering tools are required in order to shorten the total development cost of HEVs. As a matter of fact, consistent reductions in the retail price of HEVs are required in order to promote the widespread adoption of these vehicles in the market [14][15]. In this framework, a compelling need can be stated in promoting

innovative tools to rapidly evaluate design options and parameters of HEV architectures. Generally, when assessing HEV design options in early vehicle development phases, the fuel economy potential is evaluated by implementing off-line HEV powertrain energy management strategies in which the target driving mission profiles are known a priori before running the numerical simulation. Then, the selected energy management algorithm predicts the optimal fuel consumption value by optimizing the powertrain operation (e.g. gear number engaged, torque split) in the entire retained driving mission. A relevant off-line HEV energy management strategy must also demonstrate capability of effectively producing an appropriate behavior of the hybrid powertrain in terms of drivability and comfort. This translates as example in limiting the overall number of ICE activations, the number of gear shifts and the ICE speed oscillations.

Dynamic Programming (DP) currently represent the most popular HEV off-line control approach and it is generally adopted in these procedures [16][17]. The major strengths of DP relate to both its capability of returning a global optimal fuel economy solution and its flexible application to various HEV architectures including both SGT and eVT types [18][19]. Nevertheless, a major drawback of DP can be identified in its significant computational cost. This currently represents a main restriction in design methodologies implemented in HEV computer-aided engineering tools, forcing designers to restrain the amount of either the considered driving missions or the examined powertrain design parameters [20]. Moreover, as DP suffers from curse of dimensionality, its computational power and time exponentially increase when considering additional state variables to comply with further criteria in the HEV control (e.g. number of gear shifts, number of ICE activations). To solve the aforementioned issue, a recent trend can be observed in developing HEV off-line energy management strategies capable of producing a good approximation of the global optimal DP results while simultaneously limiting the related computational cost. One of the best known near-optimal HEV control approaches in this framework is represented by the Pontryagin’s Minimum Principle (PMP), which operates a local optimization considering a dual-term cost function [21]. Particularly, the instantaneous rate of fuel consumption and the employed battery power, weighted through an equivalence factor, are considered in the cost function in this case [22]. The PMP has been demonstrated to rapidly produce results comparable to DP for some retained HEV case studies [23]. Nevertheless, its implementation in HEV design methodologies requires recurrent tuning of the equivalence factor in order to achieve the charge-sustained battery operation for the analyzed driving mission [24]. Moreover, limiting the number of ICE activations over time in PMP involves implementing and tuning a dedicated ICE command filter [25]. In general, when further enhancing HEV drivability and comfort, each evaluation criterion would thus require developing a corresponding additional filter in PMP. These represent demanding procedures since the calibration process for the equivalence factor and the command filters must be repeated not only for each considered drive cycle, but also for each analyzed design option. Moreover, the near-optimality of PMP may be compromised depending on the influence of the developed command filters and on the specific powertrain operating conditions. Three additional rapid near-optimal HEV off-line control techniques, named the power-weighted efficiency analysis for rapid sizing (PEARS), the efficiency evaluation real-time control strategy (EERCS) and the slope-weighted energy-based rapid control analysis (SERCA), have been introduced by Zhang et al. in 2013 [26], by Qin et al. in 2018 [27], and by the authors of this paper in 2019 [28], respectively. As it will be described in par. 3.2, these heuristic optimization algorithms operate by iteratively replacing pure electric with hybrid operation in the most convenient time points of the driving mission until the charge-sustained battery operation is achieved. PEARS, EERCS and SERCA have been proved to generate fuel economy results comparable to DP while limiting the associated computational cost. Furthermore, computationally efficient approaches to enhance drivability and comfort have been demonstrated implementable within these HEV control strategies [29]. Nevertheless, the application of PEARS, EERCS and SERCA is currently limited to eVT HEVs only [30][31].

As a main outcome of this literature analysis, an effective off-line control strategy capable of rapidly predicting the fuel economy capability of SGT HEVs while accounting for drivability criteria still requires development. A crucial need for implementing computationally efficient near-optimal off-line control strategies for SGT HEV layouts can therefore be identified in order to fulfil the highlighted research gap. These strategies should be able to rapidly assess the fuel economy capability of SGT HEVs while considering drivability and comfort related to the generated powertrain control actions. Particularly for SGT HEVs, ensuring smooth driving might translate into effectively limiting the number of ICE activations and gear shifts as example. To answer these needs, this paper proposes a computationally lightweight off-line HEV control strategy that can assess the near-optimal fuel economy capability of SGT HEVs and increase vehicle drivability. The main contributions of this paper compared to the current state-of-art include (1) the development of a version of the SERCA algorithm capable of rapidly estimating the fuel economy capability of SGT HEVs, (2) the implementation of a dedicated approach to optimally minimize both the number of ICE activations and gear shifts throughout considered driving missions, (3) a comparative analysis of SERCA and DP control approaches applied to SGT HEVs by varying the retained number of state variables. By comparing values for the estimated fuel consumption, the number of ICE activations and gear shifts occurring throughout various driving missions, the SERCA algorithm demonstrates a satisfactorily accurate approximation of the global optimal solution provided by DP while remarkably reducing the associated computational cost. In general, the developed SERCA algorithm could find implementation in design and sizing methodologies for SGT hybrid electric powertrains to accelerate the overall vehicle development process.

The rest of the paper is organized as follows: the two considered SGT HEV architectures that include a single-motor parallel P2 layout and a dual-motor series-parallel P1P2 layout are firstly reviewed in section 2. The adopted modeling approach is described as well in this section. Then, the state-of-art off-line HEV control is discussed in section 3 considering both the global optimal energy management through DP and the rapid near-optimal energy management with SERCA and PEARS. The section 4 aims at illustrating and detailing the dedicated version of the SERCA algorithm for SGT HEVs. Simulation results are then illustrated in section 5to prove the effectiveness of the developed algorithm considering both a sensitivity study and a benchmark study. Finally, conclusions are given in section 6.

2. Parallel and series-parallel HEV layouts

This section aims at illustrating the SGT HEV layouts retained in this study and the correspondingly adopted modeling approach. A single-motor parallel P2 architecture and a dual-motor series-parallel P1P2 architecture are particularly considered.

2.1. Parallel P2 HEV

Fig. 1 illustrates a parallel P2 HEV layout. As it can be seen, the torques of ICE and MG are additive and governed by the following equation:

$$T_{ICE} + T_{MG} = T_{AT} \quad (1)$$

T_{ICE}, T_{MG}, and T_{AT} refer to the ICE torque, the MG torque, and the torque at the automatic transmission input shaft, respectively. Gear shifting in the automatic transmission is enabled by $Clutch_2$, while $Clutch_1$ ensures the connection of the ICE to the driven wheels and allows engine cranking operations. As reported in Table 1, three operating modes are available for this HEV architecture, named pure electric, torque assist and battery charging. Different operating modes are enabled depending whether the ICE is activated and employed to propel the vehicle or not and according to the value of T_{ICE}. In torque assist mode, both T_{ICE} and T_{MG} are positive and the overall torque provided to the transmission shaft is represented by the sum of their partial contributions. In battery charging mode, the ICE provides higher torque compared to the amount of torque requested by the driver. The exceeding torque value is then absorbed by the MG, which operates as generator to charge the battery.

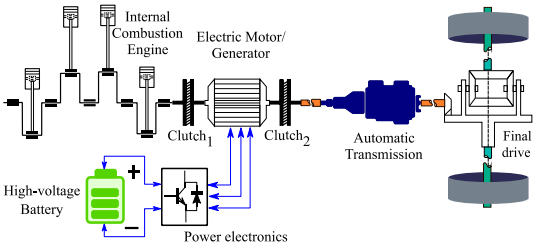

Fig. 1. Parallel P2 HEV powertrain layout.

Table 1

Operating modes of the parallel P2 HEV layout

Mode	Clutch 1	ICE	T_{ICE}	T_{MG}
Pure electric	Disengaged	OFF	$T_{ICE} = 0$	$T_{MG} = T_{AT}$
Torque assist	Engaged	ON	$T_{ICE} < T_{AT}$	$T_{MG} > 0$
Battery charging	Engaged	ON	$T_{ICE} > T_{AT}$	$T_{MG} < 0$

2.2. Series-parallel P1P2 HEV

Fig. 2 illustrates the series-parallel P1P2 HEV layout. Compared to the P2 architecture described in the previous paragraph, in this HEV an additional MG is located downstream the ICE on its same shaft. The electric path that connects the high-voltage battery through the power electronics to the electric machines thus depends on the sum of the torque values of both MGs. The torque balance equation can be rewritten considering T_{MG2} as an additional term for the MG2 torque:

$$T_{ICE} + T_{MG1} + T_{MG2} = T_{AT} \quad (2)$$

Table 2 reports the operating modes of the P1P2 HEV layout. In addition to the three operating modes of the P2 architecture, a series mode is enabled as well in the P1P2 HEV layout when an appropriate ratio between MG1 size and ICE size is accomplished. In the series mode, the ICE is activated and only MG2 propels the vehicle while the MG1 operates as generator in order to either charge the battery or allow the battery to operate in higher efficiency.

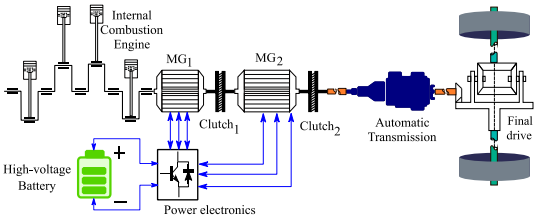

Fig. 2. Series-parallel P1P2 HEV powertrain layout.

Table 2

Operating modes of the series-parallel P1P2 HEV layout

Mode	$Clutch_1$	ICE	T_{ICE}	T_{MG1} ; T_{MG2}
Pure electric	Disengaged	OFF	$T_{ICE} = 0$	$T_{MG1} = 0$; $T_{MG2} = T_{AT}$
Torque assist	Engaged	ON	$T_{ICE} < T_{AT}$	$(T_{MG1} + T_{MG2}) > 0$
Battery charging	Engaged	ON	$T_{ICE} > T_{AT}$	$(T_{MG1} + T_{MG2}) < 0$
Series	Disengaged	ON	$T_{ICE} > 0$	$T_{MG1} = -T_{ICE}$; $T_{MG2} = T_{AT}$

2.3. HEV modeling approach

In this paper, both the considered SGT HEV architectures are modelled through the well-known backward quasi-static approach [32]. This method considers adjacent values of the simulated driving mission speed profile to calculate the amount of propelling or braking torque requested at the wheels (T_{wheels}) backwards as follows:

$$T_{wheels} = \left(F_{roll} + F_{misc} + F_{aero} + m_{veh_{eq}}(n_{gear}) \cdot a\right) \cdot r_{wheel} \quad (3)$$

With: $F_{roll} = m_{veh} \cdot g \cdot f_0$

$F_{misc} = m_{veh} \cdot g \cdot \sin(\alpha) + k \cdot v$

$F_{aero} = \frac{1}{2} \cdot \rho \cdot S \cdot C_x \cdot v^2$

F_{aero}, F_{misc} and F_{roll} represent resistive load terms provided by aerodynamic drag, some miscellaneous terms (e.g. transmission losses, side forces, road slope) and the rolling resistance, respectively. a relates to the value of vehicle acceleration or deceleration as requested by the

analysed time point in the driving mission. m_{veh}, r_{wheel} and $m_{veh_{eq}}$ are vehicle mass, wheel effective radius and vehicle equivalent mass, respectively. Particularly $m_{veh_{eq}}$ considers both the inertia of the powertrain rotating components (wheels, shafts, ICE and MGs) and the value of gear ratios for the gear engaged n_{gear}. g, α and ρ stand for the gravity's acceleration, the road slope and the air density, respectively. f_0, k, S and C_x represent vehicle parameters corresponding to the rolling friction coefficient, a miscellaneous loss coefficient, the frontal area and the drag coefficient, respectively.

Then, the torque at the automatic transmission input shaft T_{AT} can be determined as follows by evaluating the torque balance between input and output of the automatic transmission:

$$T_{AT} = T_{out} \cdot \frac{i_{FD} \cdot i_{n_{gear}}}{(\eta_{FD} \cdot \eta_{AT})^{sign(T_{out})}} \quad (4)$$

i_{FD} and $i_{n_{gear}}$ represent the gear ratio values for the final drive and the engaged gear number, respectively. η_{FD} and η_{AT} are the efficiency values for the final drive and the automatic transmission gearbox respectively, which are considered as constant values in this paper. These two latter parameters are powered to the sign of the output torque in order to account for both propelling and braking cases.

Concerning the power components, these are modelled through their empirical operational lookup tables. Particularly, the fuel map and the electric loss tables with torque and speed as independent variables are considered to represent the ICE fuel consumption and the electrical losses for each MG, respectively. Once the total amount of electrical power exchanged between power components and battery is evaluated (P_{batt}), the corresponding variation in the state-of-charge (SOC) is calculated. This term ($\dot{SOC}$) can be determined as follows by considering an equivalent open circuit model for the battery:

$$\dot{SOC} = \frac{V_{OC}(SOC) - \sqrt{V_{OC}(SOC)^2 - 4 \cdot R_{IN}(SOC) \cdot P_{batt}}}{2 \cdot R_{IN} \cdot Q_{batt}} \quad (5)$$

R_{IN}, V_{OC} and Q_{batt} represent the internal resistance, the open-circuit voltage and the capacity of the battery (in ampere-second), respectively. Both the values of R_{IN} and V_{OC} are function of the current battery SOC value according to empirical lookup tables. However, averaged constant values are considered here for these two parameters as this has been proved an appropriate approximation when studying charge sustained HEV control problems [23].

The main advantage of the backward quasi-static approach relates to its computational efficiency. This method is consequently adopted in early phases of the HEV architecture selection and powertrain design process. Indeed, considering transient phenomena and high-fidelity powertrain models at this point would dramatically increase the computational cost required for the preliminary HEV analysis. Here, both the illustrated vehicle and powertrain model and the HEV control strategies are implemented in MATLAB© software.

3. Optimal HEV off-line control

In this section, the off-line HEV control problem is discussed. Off-line control is commonly adopted to analyze the behavior of HEV architecture and sizing candidates in different pre-selected driving missions (both type-approval drive cycles and real-world driving profiles). The fuel economy capability of each retained design option is assessed in this way. The off-line HEV control problem can be formulated as follows:

$$\min\left\{ J = \int_{t_0}^{t_{end}} L(t)dt \right\}$$

with:

$$L = \dot{m}_{fuel} + \alpha_1 \cdot ICE_{start} + \alpha_2 \cdot gear_{shift}$$

subject to:

$$\begin{gathered} n_{gear_{min}} \leq n_{gear} \leq n_{gear_{MAX}} \\ \omega_{ICE_{min}} \leq \omega_{ICE} \leq \omega_{ICE_{MAX}} \\ T_{ICE_{min}} \leq T_{ICE} \leq T_{ICE_{MAX}} \\ \omega_{MG1_{min}} \leq \omega_{MG1} \leq \omega_{MG1_{MAX}} \\ T_{MG1_{min}} \leq T_{MG1} \leq T_{MG1_{MAX}} \\ \omega_{MG2_{min}} \leq \omega_{MG2} \leq \omega_{MG2_{MAX}} \\ T_{MG2_{min}} \leq T_{MG2} \leq T_{MG2_{MAX}} \\ \dot{SOC} = f(SOC, \omega_{MG1}, T_{MG1}, \omega_{MG2}, T_{MG2}) \\ SOC(t_0) = SOC(t_{end}) \\ SOC_{min} < SOC < SOC_{MAX} \end{gathered} \quad (6)$$

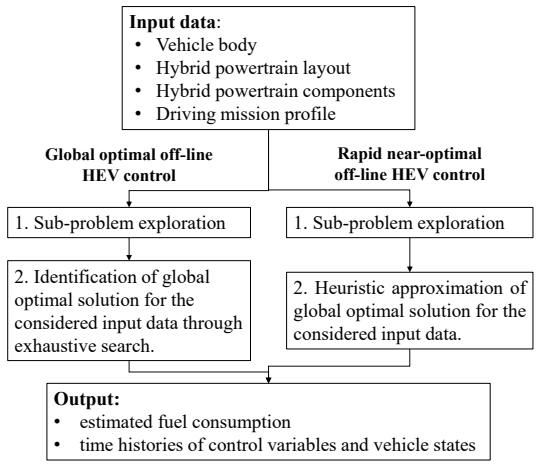

Fig. 3. Relationship between global optimal HEV control and rapid near-optimal HEV control.

L is the instantaneous cost function which needs minimization. $\dot{m}_{fuel}$ represents the instantaneous rate of fuel consumption as given by the ICE fuel table, while ICE_{start} and $gear_{shift}$ denote ICE activation and gear shifting events, respectively. α_1 and α_2 are constant weighting factors. Both gear number (n_{gear}), speeds (ω) and torques (T) are constrained within the corresponding allowed limits. Equal battery SOC values are imposed at the beginning and at the end of the considered driving mission in order to achieve the charge sustained HEV powertrain operation. Solving the introduced control problem leads to determine the evolution over time of control actions associated to the specific HEV layout. These control actions relate to the values assumed by the control variables. For the parallel P2 HEV layout illustrated in Fig. 1, the control variable set U_{P2} includes the choice of the gear number to engage and the value of T_{ICE}:

$$U_{P2} = \begin{Bmatrix} n_{gear} \\ T_{ICE} \end{Bmatrix} \tag{7}$$

In a backward approach, knowing T_{ICE} indeed allows to directly determine T_{MG} through (1). As consequence, pure electric, torque assist and battery charging operating modes can be automatically defined by a zero value of T_{ICE}, a value of T_{ICE} less than the requested transmission torque and a value of T_{ICE} greater than the requested transmission torque, respectively. As regards the P1P2 HEV layout, the related control variable set U_{P1P2} can be defined as follows:

$$U_{P1P2} = \begin{Bmatrix} n_{gear} \\ T_{ICE} \\ T_{MG1} \\ \omega_{ICE} \\ Cl_1 \end{Bmatrix} \tag{8}$$

Cl_1 is a binary variable that states if clutch$_1$ is engaged or disengaged. In case clutch$_1$ is engaged, the value of T_{MG2} can be computed from the values of T_{MG1} and T_{ICE} according to (2). When clutch$_1$ is disengaged, pure electric mode or series mode are activated depending on T_{ICE} being zero or positive. If series mode is selected, ω_{ICE} is required as additional variable to control the speed of the shaft connected to ICE and MG1. It should be noticed that, when clutch$_1$ is engaged, ω_{ICE} represents a redundant variable since the speed values for all the components are automatically determined by the wheel shaft speed and the selected gear ratio. On the other hand, if clutch$_1$ is disengaged, a different redundant control variable can be associated with T_{MG1} since its value can be automatically established by following the equations illustrated in Table 2.

Two different approaches for solving the illustrated control problem will be illustrated in the next paragraphs, namely global optimal control and rapid near-optimal control. The flowchart illustrating the relationship between these two methodologies is reported in Fig. 3. As it will be detailed later, both global optimal control and rapid near-optimal control firstly consider the exploration of all the possible sub-solutions (i.e. control actions) for each sub-problem (i.e. time instant) of the retained driving mission. However, while the former can return a global optimal solution by means of an exhaustive search that usually turns out to be computationally expensive, the latter can rapidly achieve a heuristic approximation of the global optimal solution.

3.1. Global optimal control

As previously introduced, DP currently represents the most adopted approach to obtain a global optimal solution for the above-mentioned HEV off-line control problem. This method requires the definition of state variables that describe the HEV state along the time horizon of the examined control problem

[33]. The HEV state variables adopted here can be defined as follows:

$$X = \begin{Bmatrix} SoC \\ ES \\ n_{gear} \end{Bmatrix} \quad (9)$$

Where ES refers to a binary variable determining the ICE state (i.e. on/off). ES and n_{gear} are particularly considered here to detect ICE activations and gear shifts. For passenger comfort reasons, both the numbers of ICE activations and gear shifting occurrences indeed need proper minimization through weighted penalization in the overall cost function implemented in (6) [34]. In DP, discretized arrays need to be defined both for the control variable set and the state variable set. The algorithm then explores the time horizon of the control problem backwardly from the last instant to the first instant. Particularly, all the possible discretized control actions and state values are exhaustively examined while solving an optimization problem that involves the last time instant, the last two ones, the last three ones, etc. until the initial time instant is reached [35].

The highlight of DP relates to its capability of producing a global optimal solution for the HEV off-line control problem. Moreover, the generic formulation of DP enables the flexible adaptation of this algorithm to various HEV architectures including both SGT and eVT layouts. However, the exhaustive search operated by DP dramatically increases the computational cost associated to this method. Despite remarkable advances have been observed lately for computational power available, current computers still require significant time for solving complex DP problems [36]. To overcome this draft, scientists and researchers worldwide have recently started developing near-optimal algorithms capable of approximating the global optimal solution provided by DP while simultaneously narrow the required computational cost. The next paragraph will provide more details about these algorithms currently under development.

3.2. Rapid near-optimal control

The motivation for developing rapid near-optimal off-line HEV control algorithms notably arose at the beginning of this decade as researchers started analyzing the design problem for multimode eVT HEVs [37]. These HEV architectures embed one or multiple planetary gear sets and they characterize by connections (either permanent or clutch-based) between different nodes of the planetary gear sets or with the ground [38]. The resulting design space can include up to billions of options when both the location of clutch connections and component sizing are retained as design parameters [39]. Moreover, since the location of both clutch-based and permanent-based connections represents a discrete design variable, brute force currently represents the only optimization procedure implementable for these HEVs [40]. In this case, analyzing each design option by means of DP would require an excessive computational time (in the order of magnitude of months to years). To mitigate this issue, Zhang et al. proposed a rapid near-optimal HEV off-line control algorithm named PEARS. In this algorithm, each time instant of the driving mission is firstly analyzed to extract the best operating point of the power components for each mode of the eVT HEV powertrain layout. The best operating points are particularly determined in order to maximize a power-weighted efficiency formulation which accounts for only the electric power (for pure electric modes) or for both the electric power and the fuel power (for hybrid modes). The HEV is then set to function in pure electric operation for the entire driving mission under analysis and the associated total electrical energy required is computed. Subsequently, a recursive procedure can be performed by replacing electric with hybrid operation in the time instant of the driving mission in which the narrowest difference is observed in the power-weighted efficiency values between the best electric mode and the best hybrid mode of the HEV powertrain. This operation is iterated until the electrical energy required to complete the rest of the driving mission in pure electric operation reaches a zero or negative value. The charge sustained HEV operation is achieved in this way. The PEARS algorithm has been successfully applied to multimode eVT HEVs and it has been demonstrated predicting fuel economy capability results comparable to the ones of DP while reducing the associated computational time by three to four orders of magnitude [26]. The authors of this paper then

introduced an improved version of the PEARS algorithm which included the minimization of mode-shifting occurrence throughout the analyzed driving mission. Partially accounting for ride comfort in these rapid preliminary HEV analysis as well was made possible in this way [29]. However, when attempting to implement the PEARS algorithm to rapidly control a dual-mode eVT HEV from the industrial state-of-art, the authors of this paper realized that this algorithm was underperforming with respect to the multimode eVT layouts. The reason for this drawback was associated to the PEARS algorithm being originally designed for eVT HEVs with multiple operating modes rather than only one pure electric mode and one hybrid mode. This leaded to the development of a new HEV off-line control strategy named SERCA. This algorithm inherited the iterative electric-to-hybrid replacement process from PEARS. However, the single optimal operating point identification by means of the power-weighted efficiency formulation is replaced for the SERCA algorithm by a hull of optimal operating points identified by maximizing the slope between the recharged battery energy and the corresponding instantaneous fuel consumption. This enhances the flexibility of the algorithm in having further optimal hybrid operating points available at each time instant. When firstly introduced, the SERCA algorithm has been demonstrated generating results closer to DP, while exhibiting a narrow increase in the computational time compared to PEARS [28]. Even though the PEARS and SERCA techniques have been developed for eVT HEVs, not many similar approaches have been implemented so far to accelerate the fuel economy capability prediction of SGT HEVs. The next section consequently aims at introducing a dedicated formulation of the SERCA algorithm for SGT HEVs.

4. The SERCA algorithm for parallel and series-parallel HEVs

This section details the formulation of the SERCA algorithm specifically developed to advance the fuel economy prediction of both parallel and series-parallel SGT HEV layouts. For the sake of continuity, the SERCA will be described here following the same division as the algorithm for eVT HEVs: the exploration of sub-problems, the identification of the optimal operating points and the achievement of charge sustained operation. The complete pseudo-code of SERCA is detailed in Algorithm 1.

4.1. Sub-problem exploration

During step 1 of Algorithm 1, all the possible control actions are analyzed for each sub-problem (i.e. each time instant of the analyzed driving mission). Sub-problems are defined according to peculiar values of vehicle output speed and requested vehicle acceleration. A discretized array is created for each control variable in a similar way to DP. Each subproblem is subsequently explored by sweeping all the possible sub-solutions (i.e. all the combinations of the discretized values for the control variables). If a sub-solution respects all the feasibility criteria listed in (6), it represents a feasible sub-solution and it will be stored. On the other hand, solutions not meeting all the feasibility requirements are discarded. Finally, two evaluation parameters characterize each identified feasible sub-solution: the instantaneous fuel consumption and the corresponding battery SOC variation, both assessed according to the vehicle and powertrain model presented in section 2.3.

4.2. Identification of optimal operating points

After all the feasible sub-solutions have been associated with the corresponding fuel consumption and battery SOC variation, step 2 in algorithm 1 will then identify and store the optimal operating points for each sub-problem of the driving mission under study. The feasible sub-solutions for a sub-problem can be graphically organized in a 2D plot with fuel consumption and battery SOC depletion as independent variables. A related example plot is illustrated in Fig. 4 that shows sub-solutions for three different gears.

Algorithm. 1 SERCA

Input: vehicle parameters, HEV powertrain components and driving mission

Output: estimated fuel consumption, time histories of control variables and vehicle states

0: Initiate HEV control optimization

1: Sub-problems exploration

For each sub-problem i

For each sub-solution j

1.1 Check feasibility of sub-solution j

1.2 Compute fuel consumption of sub-solution j

1.3 Compute SOC variation of sub-solution j

end for

2: Identification of optimal operating points

2.1 Compute slope θ_{HEV} for each sub-solution for sub-problem i

2.2 Identify optimal sub-solution for sub-problem i

end for

3: Charge balanced analysis

3.1 Compute time history of gear number throughout the entire driving mission according to λ_{GS}

3.2 Create table of optimal sub-solutions for the driving mission $p_{sub\text{-}optimal}$

3.3 Compute required electrical energy E_{EV} for pure electric operation throughout the entire driving mission

While $E_{EV} \geq 0$

3.4 Determine sub-optimal hybrid electric sub-solution

3.4.1 Identify hybrid electric sub-solution *a* with maximum slope θ_{HEV_MAX} throughout the entire driving mission

3.4.2 Identify best hybrid electric sub-solution *b* among sub-problems adjacent to time instants already operating in hybrid electric mode $\theta_{HEV\_MAX\_adj}$

if $\theta_{HEV\_MAX\_adj} \geq \theta_{HEV\_MAX} \cdot \lambda_{ICE}$

3.4.3 Select sub-solution *b*

else

3.4.3 Select sub-solution *a*

end if

3.5 Update E_{EV}, estimated fuel consumption and time series control variables according to selected sub-solution

3.6 Delete selected sub-solution from $p_{sub\text{-}optimal}$

end while

The pure electric operating points are particularly distinguished by a zero value of fuel consumption and positive battery energy consumption. On the other hand, by enabling the hybrid operation it becomes possible to progressively decrease the SOC depletion and consequently recharge the battery while correspondingly increasing the amount of fuel consumed. With reference to [28], the same sub-solution comparison was performed for an eVT HEV that is shown in Fig. 4. Nevertheless, the same plot for a sub-problem reveals different trends according to the specific HEV layout. In the eVT HEV case, a

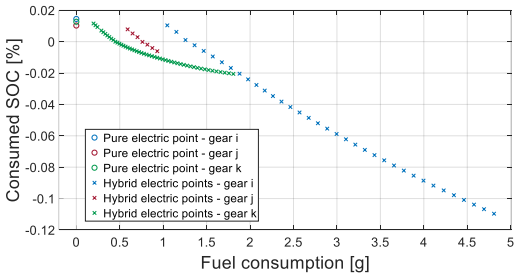

Fig. 4. Pareto frontier for sub-solutions in terms of fuel consumption and battery SOC variation for a single sub-problem (SGT HEV).

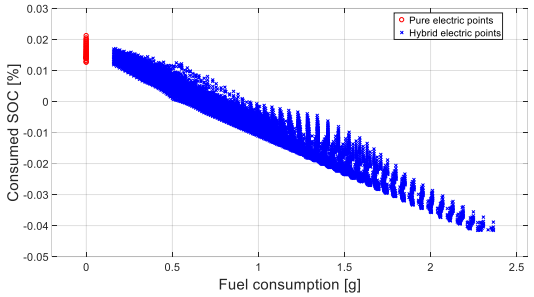

Fig. 5. Pareto frontier for sub-solutions in terms of fuel consumption and battery SOC variation for a single sub-problem (eVT HEV).

cloud of hybrid sub-solutions can be particularly established. This correlates well with the operating principle of an eVT transmission, where different sub-solutions can be associated with diverse values of ICE speed and torque. When developing this step of the SERCA algorithm for eVT HEVs, the authors of this paper consequently developed a dedicated procedure to identify the optimal sub-solutions. Three steps were particularly accomplished including a discretization of the fuel consumption interval, the identification of the optimal sub-solution for each discretized fuel consumption value, and a piecewise relaxation to ensure that the identified optimal hull exhibited a convex trend.

As it can be seen in Fig. 4, the sub-solutions comparison plot for an SGT HEV contrasts with its counterpart for an eVT HEV shown in Fig. 5. Since the ICE speed is constrained by the value of the vehicle speed associated to the sub-problem under study, a homogenous cloud of hybrid solutions is not made possible anymore. Rather, different single discretized arches can be observed that relate to the corresponding gear numbers. As consequence, a

peculiar procedure needs implementation for extending the SERCA algorithm to SGT HEVs. Here, one optimal pure electric sub-solution and multiple optimal hybrid sub-solutions are specifically identified for each sub-problem. An optimization problem can be stated whose resolution will determine $\mathrm{opt}_{\mathrm{EV}}$, the optimal pure electric sub-solution for the analyzed sub-problem.

$$\begin{aligned} \mathrm{opt}_{\mathrm{EV}} &= \min\left[\dot{SOC}\ (n_{gear})\right] \\ \text{subject to: } & \dot{m}_{fuel} = 0 \end{aligned} \tag{10}$$

The gear number related to the optimal pure electric sub-solution for each sub-problem can be thus identified, meanwhile the corresponding values of $\dot{SOC}$ are recorded. As regards the hybrid operating points, an optimal sub-solution is retained for each feasible gear number associated to the specific sub-problem. For this purpose, for each generic hybrid point HEV_k a slope value (θ_{HEV_k}) is defined that represents the highlight of the SERCA algorithm.

$$\theta_{HEV_k} = \frac{\Delta \dot{SOC}}{\Delta \dot{m}_{fuel}} = \frac{|\dot{SOC}(k) - \dot{SOC}(\mathrm{opt}_{\mathrm{EV}})|}{\dot{m}_{fuel}(k)} \tag{11}$$

The slope θ_{HEV_k} can thus be defined as the ratio between the gain in battery energy with respect to the pure electric optimal sub-solution and the correspondingly consumed fuel. For each generic feasible gear *i*, it becomes possible to determine the optimal hybrid sub-solution $\mathrm{opt}_{\mathrm{HEV}_{\mathrm{gear}_i}}$ for each sub-problem by solving the following optimization problem.

$$\begin{aligned} \mathrm{opt}_{\mathrm{HEV}_{\mathrm{gear}_i}} &= \max\left[\theta_{HEV_k}(\Delta \dot{SOC}, \dot{m}_{fuel}(k))\right] \\ \text{subject to: } & \dot{SOC}(k) \geq \dot{SOC}(\mathrm{opt}_{\mathrm{EV}}) \end{aligned} \tag{12}$$

$\mathrm{opt}_{\mathrm{HEV}_{\mathrm{gear}_i}}$ should maximize the slope between the gain in battery energy and the fuel consumption compared with $\mathrm{opt}_{\mathrm{EV}}$ selected above. The condition reported in (12) ensures that the battery energy consumption in optimal hybrid operation is reduced with respect to the pure electric counterpart. The optimal pure electric and hybrid sub-solutions are thus identified and stored for all the sub-problems of the considered driving mission in this way in the table $p_{sub\text{-}optimal}$.

4.3. Charge balanced analysis

In step 3 of Algorithm 1 for SERCA, the off-line HEV control problem illustrated in (6) is solved for the entire considered driving mission. This is achieved by analyzing the information coming from the analysis of all the sub-problems conducted above. Two sub-steps need achievement to complete the charge balanced analysis.

4.3.1 Initially, the HEV layout is scheduled to operate through the entire driving mission in pure electric mode. At this point, a trade-off is needed between energy saving and driving comfort. While the first term can be easily quantified by the amount of consumed battery energy, here the latter term is characterized by the number of gear-shifting events. Following the approach illustrated in [29], a coefficient λ_{GS} can be defined in order to reduce the gear-shifting occurrence. The following analysis, repeated for each time instant *k*, allows to determine the selected gear in pure electric operation (*gear(k)*) throughout the overall driving mission:

$$gear(k) = \begin{cases} gear_{opt_{EV}} \text{ if } \dot{SOC}_{gear_{opt_{EV}}}(k) \geq \lambda_{GS} \cdot \dot{SOC}_{gear_{k-1}}(k) \\ gear_{k-1} \text{ if } \dot{SOC}_{gear_{opt_{EV}}}(k) < \lambda_{GS} \cdot \dot{SOC}_{gear_{k-1}}(k) \end{cases} \tag{13}$$

Where $gear_{opt_{EV}}$ refers to the optimal gear number identified in (10), while $gear_{k-1}$ is the gear number selected in the previous time instant. At each time instant, the SOC rate in pure electric operation for the gear number selected at the previous time instant is computed and represented by $\dot{SOC}_{gear_{k-1}}(k)$. The illustrated methodology thus enables a gear-shifting occurrence only in case enough advantage is realized in terms of energy savings. Driving comfort is prioritized alternatively.

After the procedure is repeated for all the time instants of the driving mission (from the first one to the last one), the electrical energy required to operate the driving mission in pure electric operation (E_{EV}) is computed. This can be achieved by integrating over time the instantaneous SOC rates thorough the entire driving mission.

4.3.2 A recursive process is then performed in order to achieve charge balanced operation. Indeed, at this point of the algorithm a charge depleting scenario is defined since the ICE has never been activated thorough the driving mission. A search is particularly performed in sub-step 3.4.1 to identify the time instant in which the highest value of θ_{HEV_k} (i.e. the steepest slope) is observed. For the selected time instant, the pure electric operation is replaced with the hybrid operation corresponding to the control variable values of the sub-solution *p(j)* corresponding to the highest value of $\mathrm{opt}_{\mathrm{HEV}_{\mathrm{gear}_i}}$. The overall fuel consumption for the driving mission is then updated by adding the fuel cost related to the hybrid operation in the identified time instant. Meanwhile, E_{EV} is updated considering two energy terms for the selected time instant. Particularly, the electrical energy required for the previously defined pure electric operation is subtracted, while the electrical energy corresponding to the just selected hybrid operation is algebraically summed. After the first electric-to-hybrid replacement *j* is performed, a procedure like (13) can be implemented in the following iteration *j+1* in order to minimize the amount of ICE activation events (14) for sub-step 3.4.3. The values of θ_{HEV} for the time instants adjacent to the ones already operating in hybrid mode are particularly considered. Among them, the best sub-solution p_{adj_best} can be identified in sub-step 3.4.2 through the maximum slope $\theta_{HEV_{MAX}-adj}$. On the other hand, $\theta_{HEV_{MAX}}$ represents the highest slope identified among all remained sub-solution for the table $p_{sub\text{-}optimal}$.

$$p(j+1) = \begin{cases} p_{adj\_best} \text{ if } \theta_{HEV_{MAX}-adj} \geq \theta_{HEV_{MAX}}(j+1) \cdot \lambda_{ICE} \\ p_{best}(j+1) \text{ if } \theta_{HEV_{MAX}-adj} < \theta_{HEV_{MAX}}(j+1) \cdot \lambda_{ICE} \end{cases} \quad (14)$$

p(j+1) represents the sub-solution selected for hybrid electric operation at iteration j+1 of step 3.4 in Algorithm 1, while λ_{ICE} is a constant coefficient aiming at minimizing the number of ICE activation events. Following (14), hybrid electric operation is prioritized in the time instants adjacent to the ones already operating in hybrid mode if satisfactory overall efficiency of the HEV powertrain is maintained. Otherwise, the time instant corresponding to the best sub-solution among the remaining ones in the table $p_{sub\text{-}optimal}$ is retained, thus involving a further ICE activation event.

Each electric-to-hybrid replacement iteration is followed by a check for the value of E_{EV}. After updating the overall fuel consumption and electrical energy needed, the selected sub-solution is deleted from the table $p_{sub\text{-}optimal}$ in order not to retain it repetitively. The recursive process is then carried out until E_{EV} exhibits a zero or negative value.

Once this final step is achieved, a solution for the off-line HEV control problem can be obtained for an SGT HEV layout. The SERCA algorithm thus allows to rapidly estimate the fuel consumption of the HEV in a charge-balanced scenario over a driving mission. The reader is now invited to further refer to Fig. 5 for a graphical illustration of the workflow of the algorithm.

5. Simulation results

This section aims at presenting results for the implementation of the SERCA algorithm on the two SGT HEV layouts under consideration in this paper (i.e. the parallel HEV and the series-parallel HEV). The representative vehicle and powertrain data retained are firstly introduced. Then, results for two case studies are presented and discussed to demonstrate the effectiveness of the proposed SERCA algorithm. A comparative study between SERCA and DP is particularly performed in terms of estimated fuel consumption, computational time (CT), number of gear shifts and ICE activation events by varying the amount of considered state variables for the off-line HEV control problem. A benchmark study is then carried out to assess the performance of SERCA in terms of fuel economy prediction and computational efficiency compared to DP as global optimal control approach for both the SGT HEV layouts over different driving missions. The final part of this section aims at summarizing main findings concerning obtained results.

5.1. Representative vehicle

A representative HEV is defined here laying the foundations for the assessment of the SERCA algorithm. Table 3 particularly illustrates retained data related to vehicle body, ICE, transmission, final drive, MGs and battery. It should be noted that the representative vehicle selected in this study does not refer to any commercially available HEV, rather open-source data for the power components are selected from [41] and linearly scaled in order to become appropriate for a minivan-type HEV. Data for the vehicle body are retained from [30], while the sizes of the MGs for both the SGT HEV layouts are selected in order to obtain an hybridization factor (i.e. the ratio between the total power of the MGs and the overall power available from both ICE and MGs) of around 0.35 [42]. A 5 gears AMT layout is finally retained with corresponding efficiency values derived from [43].

Table 3

Representative vehicle data

Component	Parameter	Value
Vehicle	Mass	2238 Kg
	Wheel dynamic radius	0.358 m
ICE	Capacity	3.3 L
	Maximum power	188 kW @ 5800 rpm
	Maximum torque	320 Nm @ 4400 rpm
Transmission	Gear ratios	[3.85 2.27 1.52 1 0.81]
	Efficiency	0.95
Final drive	Gear ratio	3.70
	Efficiency	0.95
MG (P2)	Maximum power	95 kW
MG1 (P1P2)	Maximum power	40 kW
MG2 (P1P2)	Maximum power	45 kW
Battery	Open circuit voltage	355 V
	Resistance - charging	103 mΩ
	Resistance - discharging	128 mΩ
	Capacity	6.5 Ah

5.2. Comparative study

In this first case study, a comparative analysis is performed considering SERCA and DP and varying the amount of state variables. The operating principle of DP involves the determination of a discretized state space to account for the evolution over time of vehicle states throughout the driving mission under analysis. On the other hand, the HEV off-line optimization achieved by SERCA does not require the definition of a state space, as it has been described in the previous section. Rather, dedicated approaches characterized by the usage of constant coefficients (e.g. λ_{GS}) have been illustrated in (13) and (14) to limit the variation of state variable values. Three state variables are considered in this paper for the DP optimization, i.e. battery SOC, ICE state and gear number engaged as reported in (9). Battery SOC represents an indispensable variable, since charge sustained operation could not be achieved otherwise. On the other hand, ES and n_{gear} are auxiliary, yet necessary, state variables that help accounting for drivability and smooth operation of the hybrid electric powertrains. Similarly, λ_{GS} and λ_{ICE} have been introduced in the proposed formulation of SERCA for parallel and series-parallel HEV architectures.

This comparative study firstly aims at verifying the near-optimality of the estimated fuel consumption (EFC) obtained by means of SERCA. Moreover, variations in the EFC, the CT, the number of ICE activations and the number of gear shifts are assessed when gradually increasing the number of state variables considered. Parameters for state variables of

Table 4

Parameters for state variables used in comparative study

	DP	SERCA
1 state	SoC	$\lambda_{ICE} = 1$; $\lambda_{GS} = 1$
2 states	SoC, ES	Sweep λ_{ICE} ; $\lambda_{GS} = 1$
3 states	SoC, ES, n_{gear}	Sweep λ_{ICE} ; sweep λ_{GS}

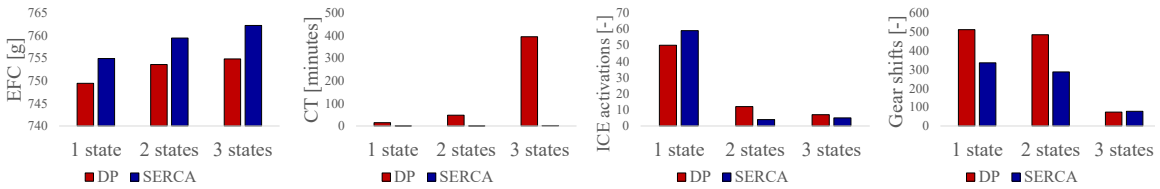

Fig. 6. Histograms for EFC, CT, ICE activations and gear shifts for parallel P2 HEV controlled by SERCA and DP in WLTP.

Table 5

Results for EFC, CT, ICE activations and gear shifts for parallel P2 HEV controlled by SERCA and DP in WLTP.

	1 state (*SOC*)		2 states (*SOC, ES*)		3 states (*SOC, ES, n_{gear}*)	
	SERCA	DP	SERCA	DP	SERCA	DP
EFC [g]	754.9	749.5	759.4	753.6	762.2	754.8
CT [minutes]	0.1	14.8	0.3	47.9	2.4	394.4
ICE activations [-]	59	50	4	12	5	7
Gear shifts [-]	335	511	287	484	78	74

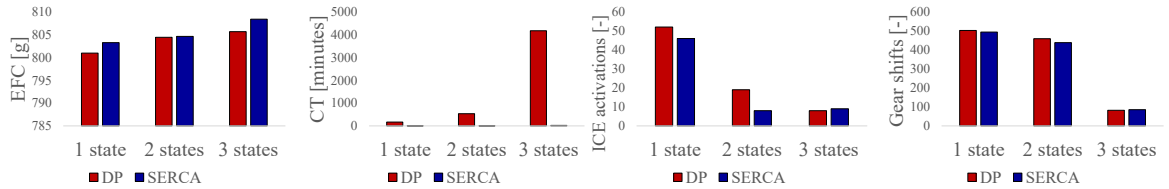

Fig. 7. Histograms for EFC, CT, ICE activations and gear shifts for series-parallel P1P2 HEV controlled by SERCA and DP in WLTP.

Table 6

Results for EFC, CT, ICE activations and gear shifts for series-parallel P1P2 HEV controlled by SERCA and DP in WLTP.

	1 state (*SOC*)		2 states (*SOC, ES*)		3 states (*SOC, ES, n_{gear}*)	
	SERCA	DP	SERCA	DP	SERCA	DP
EFC [g]	803.3	801.0	804.6	804.4	808.4	805.7
CT [minutes]	0.4	167.2	2.3	534.1	22.6	4172.5
ICE activations [-]	46	52	8	19	9	8
Gear shifts [-]	484	502	438	459	85	82

performed analysis are reported in Table 4. In the 1 state simulation, SOC is retained as the only state variable for DP, while both λ_{GS} and λ_{ICE} are set to 1 for SERCA (i.e. neither gear shifts nor ICE activations are minimized). In the 2 states simulation, ES is added as state variable in DP, while SERCA is run several times while sweeping different values of λ_{ICE} to minimize the cost function L expressed in (6). Finally, in the 3 states simulation, n_{gear} is included as well as state variable in DP, while a further sweep of values for λ_{GS} is performed in SERCA to achieve gear shifting minimization. Here, simulations are performed in the worldwide harmonized light-vehicle test procedure (WLTP). Concerning DP, SOC state vectors comprised of 2000 elements are considered, while maximum and minimum SOC values have been set to +5% and -5% with respect to the initial SOC value, respectively. Considered values for λ_{GS}

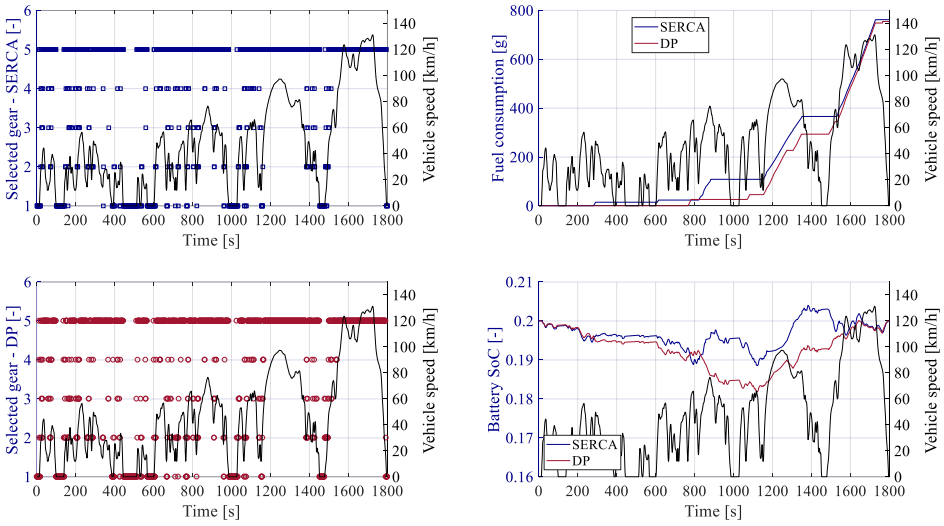

Fig. 8. Comparison of time histories of selected gear, fuel consumption and battery SoC for parallel P2 HEV controlled by SERCA and DP in WLTP.

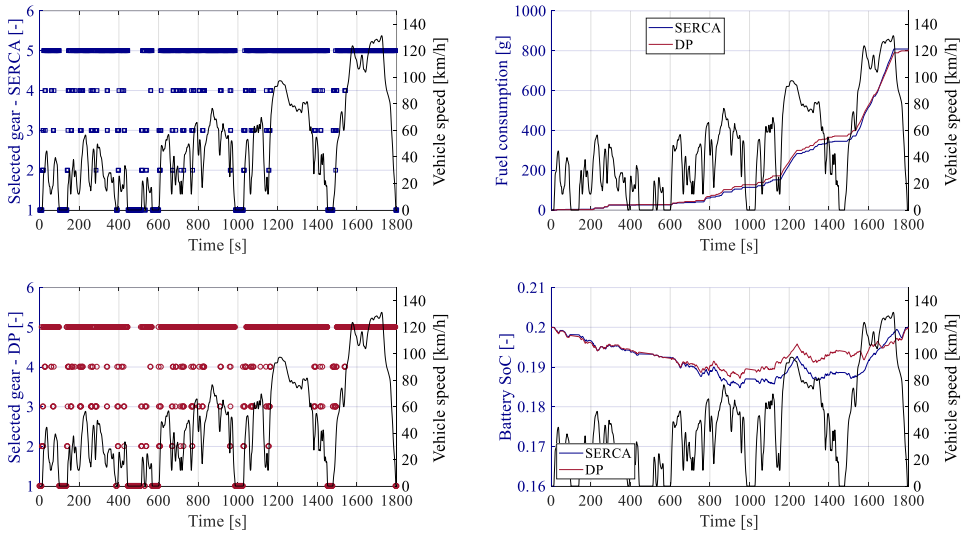

Fig. 9. Comparison of time histories of selected gear, fuel consumption and battery SoC for series-parallel P1P2 HEV controlled by SERCA and DP in WLTP.

and λ_{ICE} range from 0.1 to 1 in a discretized array comprising 20 elements.

Corresponding results are illustrated in Fig. 6 and Fig. 7 and reported in Table 5 and Table 6 for the parallel P2 and the series-parallel P1P2 HEV layout, respectively. Values of CTs here relate to a desktop computer with Intel Core i7-8700 (3.2 GHz) and 32 GB of RAM. Overall, it can be noticed how values for the EFC slightly increase when considering additional state variables. However, this corresponds to a remarkable reduction of both gear shifts and ICE activations. As example, for DP EFC increase by 0.7 % and by 0.6 % from the 1 state analysis to the 3 states analysis for P2 and P1P2 HEV layouts,

respectively. At the same time, the corresponding numbers of gear shifts reduce by 85.3 % and by 68.7 % for P2 HEV and P1P2 HEV respectively, while the ICE activation events decrease by 86.0 % and by 84.6 % for P2 HEV and P1P2 HEV respectively. In this framework, SERCA appears achieving comparable performance with respect to DP both in terms of EFC, ICE activations and gear shifts. Increase in the EFC for SERCA is indeed contained within 0.4 % and 1 % for P2 and P1P2 HEV layouts, respectively, while difference in the number of ICE activations and gear shifts are respectively limited within 2 and 4 for the P2 HEV in the 3 states analysis, and within 1 and 3 for the P1P2 HEV. The main advantage of the implementation of SERCA relates to the overall constancy in values of CT when gradually increasing the number of state variables considered. Compared to the 1 state analysis, CTs required to execute DP in 2 states and 3 states analysis are indeed 3.3 and 26.8 times respectively for the P2 HEV, and 3.2 and 25 times respectively for the P1P2 HEV. This appears in line with the well-known curse of dimensionality of DP when increasing the number of considered state variables. Moreover, overall required CTs for DP in the 3 states analysis amount to more than 6 hours and 69 hours for the P2 and the P1P2 HEV layout, respectively. These values of CT currently weaken the successful application of DP to enhanced HEV powertrain design and sizing methodologies. In this framework, the introduction of the SERCA algorithm brings considerable benefits in terms of computational cost since its CT only represents 0.6 % and 0.5 % of the CT required by DP to simulate the P2 HEV and the P1P2 HEV, respectively. Moreover, the implemented tuning process for λ_{ICE} and λ_{GS} reveals a computationally efficient way for limiting the number of ICE activations and gear shifts. Indeed, even when considering 3 state analyses, the overall CT required by SERCA is limited below 3 minutes and 23 minutes for the P2 layout and the P1P2 layout respectively.

Finally, Fig. 8 and Fig. 9 report comparisons of vehicle states (i.e. gear engaged, cumulated fuel consumption and battery SOC) according to SERCA and DP off-line control for the P2 HEV and the P1P2 HEV, respectively, considering the 3 states analysis. Overall, these results demonstrate the capability of SERCA of producing a good approximation of the global optimal control actions provided by DP, while correspondingly achieving a remarkable reduction in the required computational cost.

5.3. Benchmark study

This last results-sub-section aims at providing an exhaustive benchmark analysis between SERCA and DP over different driving missions. In addition to the WLTP, driving missions considered here include the urban dynamometer driving schedule (UDDS), the highway fuel economy test (HWFET), the new European driving cycle (NEDC) and the US06 Supplemental Federal Test Procedure (US06). Related numerical results are displayed in Table 7 and in Table 8 for the parallel P2 and the series-parallel P1P2 HEV layouts, respectively.

Overall, these results represent a further demonstration of the capabilities of the SERCA algorithm concerning the rapid near-optimal off-line HEV control. Indeed, for the selected driving missions the EFC values provided by SERCA are on average only 1.3 % and 0.3 % far from the EFC global optimal solution provided by DP for the P2 and the P1P2 HEV layouts, respectively. On the other hand, the corresponding advantage of SERCA amounts to 99.4 % and 99.5 % averaged savings in terms of CT.

5.4. Main findings

In general, avoiding the exhaustive exploration of all the possible control actions represents the main contribution to the CT reduction in SERCA. Rather, a near-optimal approximation of the global optimum HEV powertrain behavior is achieved by means of the introduced slope-based approach. The effectiveness of the proposed algorithm has been demonstrated by analyzing its operation over various drive cycles and benchmarking its performance with the global optimal benchmark provided by DP. Moreover, the introduced SERCA algorithm allows considering not only fuel economy when off-line controlling SGT HEV powertrains, but also drivability and comfort. Related metrics, such as the number of ICE activations and gear shifts as example, have not usually been considered in previous studies implementing design oriented HEV

Table 7

EFC and CT for DP and SERCA over various driving missions – parallel P2 HEV layout

	DP		SERCA	
	EFC [g]	CT [min]	EFC [g]	CT [min]
WLTP	754.8	394.4	762.5 (+ 1.6 %)	2.4 (- 99.4 %)
UDDS	266.0	312.2	271.8 (+ 2.2)	1.7 (- 99.5 %)
HWFET	555.4	168.9	558.2 (+ 0.5 %)	1.1 (- 99.3 %)
NEDC	297.2	254.3	303.2 (+2.0 %)	1.4 (- 99.5 %)
US06	517.5	131.1	522.6 (+ 1.0 %)	0.9 (-99.3 %)

Table 8

EFC and CT for DP and SERCA over various driving missions – series-parallel P1P2 HEV layout

	DP		SERCA	
	EFC [g]	CT [min]	EFC [g]	CT [min]
WLTP	805.7	4172.5	806.3 (+ 0.1 %)	22.6 (- 99.5 %)
UDDS	287.0	3181.3	287.8 (+ 0.3 %)	15.9 (- 99.5 %)
HWFET	471.3	1793.8	471.9 (+ 0.2 %)	10.8 (- 99.4 %)
NEDC	323.4	2715.9	326.5 (+ 1.0 %)	12.6 (- 99.5 %)
US06	531.5	1423.5	532.0 (+ 0.1 %)	8.3 (- 99.4 %)

off-line control strategies. As a result, many previous works were not able to generate smooth HEV driving conditions. As example, in the time domain results from DP provided by Yang et al. in 2016 for a P2 HEV in NEDC, frequent ICE activations and oscillations of speed of components due to frequent gear shifts can be observed [44]. Similarly, the operating mode selected by the DP version from Zhou et al. in 2017 for parallel P2 and multimode eVT layouts presented frequent shifts in UDDS [45]. Both these last works did not explicitly mention the number of ICE activations and gear shifts operated over time by DP. As previously mentioned, Hou et al. implemented an ICE command filter to avoid frequent engine activations when controlling a P2 HEV using PMP. However, their control approach did not allow optimizing gear shifting as well, the latter being controlled by a heuristic approach instead [25]. On the other hand, SERCA allows flexibly optimizing gear shifting, ICE activations and power split in SGT HEV powertrains at the same time. Furthermore, the implemented control approach could help avoiding the generation of irregular HEV control actions over time that might often compromise the drivability and result unfeasible from hybrid powertrains in real world.

It should be admitted that, similarly to the PMP, the proper operation of the SERCA algorithm depends on tuning of few coefficients (e.g. the gear-shifting minimization coefficient and the ICE activation minimization coefficient). However, the rapidness of SERCA allows the agile tuning process for these coefficients. Moreover, compared to the PMP, the SERCA approach enables a more flexible handling of control variables of different types (e.g. both continuous and discrete).

6. Conclusions

This paper introduces a formulation of the SERCA algorithm that enables the rapid prediction of the fuel economy capabilities of SGT HEVs. After parallel and series-parallel HEV layouts have been recalled, the algorithm has been described in its different operating steps: the exploration of sub-problems, the identification of the optimal operating points and the achievement of the charge sustained operation. Simulation results show that the SERCA algorithm can achieve EFC values close to the global optimal benchmark provided by DP by limiting the related numerical difference below around 0.1% to 2%. On the other hand, the SERCA algorithm is proved to remarkably shorten the computational cost demanded to solve the HEV off-line control problem for SGT HEV layouts. DP would indeed require

approximately a one to two orders of magnitude greater computational time to return results comparable to SERCA in terms of EFC, number of ICE activations and number of gear shifts for the retained case studies.

The rapidness and simultaneous near-optimal EFC performance of the algorithm makes SERCA appealing for various applications constituting possible future work related to this paper. First, SERCA could be straightforwardly implemented in current SGT HEV design methodologies. This would allow designers to efficiently increase both the amount of design options considered and the number of different driving missions evaluated. Moreover, the SERCA algorithm could enhance the calibration of current on-line heuristic HEV control strategies by rapidly producing off-line-optimized benchmark time series for the control variables. Finally, the development of on-line HEV controllers based on artificial intelligence could be fostered by the SERCA algorithm. Particularly, the capability of SERCA of promptly generating a considerable amount of off-line optimized data could be exploited to smoothly train and ameliorate artificial intelligences to control HEVs.

References

[1] B. Bilgin, P. Magne, P. Malysz, Y. Yang, V. Pantelic, M. Preindl et al., "Making the Case for Electrified Transportation", IEEE Transactions on Transportation Electrification 2015; 1(1): 4-17.

[2] N. Onat, M. Kucukvar, O. Tatari, “Conventional, hybrid, plug-in hybrid or electric vehicles? State-based comparative carbon and energy footprint analysis in the United States”, Applied Energy 2015; 150: 36-49.

[3] A. Emadi, “Transportation 2.0”, IEEE Power and Energy Magazine 2011; 9(4): 18-29.

[4] L. Damiani, M. Repetto, A.P. Prato, “Improvement of powertrain efficiency through energy breakdown analysis”, Applied Energy 2014; 121:252-63.

[5] R.T. Doucette, M.D., McCulloch, “Modeling the prospects of plug-in hybrid electric vehicles to reduce CO2 emissions”, Applied Energy 2011; 88(7): 2315-23.

[6] Y. Yang, K. Arshad-Ali, J. Roeleveld, and A. Emadi, “State-of-theart electrified powertrains-hybrid, plug-in, and electric vehicles”, Int. J. Powertrains 2016; 5(1): 1-29.

[7] Lee, S., Lee, B., McDonald, J., Sanchez, L., Nam, E., "Modeling and Validation of Power-Split and P2 Parallel Hybrid Electric Vehicles," SAE Technical Paper 2013-01-1470, 2013.

[8] Y. Yang, N. Schofield, A. Emadi, "Integrated Electromechanical Double-Rotor Compound Hybrid Transmissions for Hybrid Electric Vehicles", IEEE Transactions on Vehicular Technology 2016; 65(6): 4687-99.

[9] T. Hutchinson, S. Burgess, G. Herrmann, “Applying empiricaldesign data to life cycle assessment and whole-life cost analysis”, Applied Energy 2014; 119: 314-329.

[10] Matsumura, M., Shiozaki, K., and Mori, N., “Development of New Hybrid Transaxle for Mid - Size Vehicle,” SAE Technical Paper 2018-01-0429, 2018.

[11] W. Zhuang, S.L. Eben, X. Zhang, D. Kum, Z. Song, G. Yin, J. Ju, “A survey of powertrain configuration studies on hybrid electric vehicles”, Applied Energy 2020; 262: 114553.

[12] R. Finesso, E. Speesa, M. Venditti, “Cost-optimized design of a dual-mode diesel parallel hybrid electricvehicle for several driving missions and market scenarios”, Applied Energy 2016; 177: 366-383.

[13] Kapadia, J., Kok, D., Jennings, M., Kuang, M., Masterson, B., Isaacs, R. et al., "Powersplit or Parallel - Selecting the Right Hybrid Architecture," SAE Int. J. Alt. Power 2017;. 6(1): 68-76.

[14] K. Palmer, J. Tate, Z. Wadud, J. Nellthorp, “Total cost of ownership and market share for hybrid and electric vehicles in the UK, US and Japan”, Applied Energy 2018; 209: 108-19.

[15] B. Al-Alawi, T. Bradley, “Total cost of ownership, payback, and consumer preference modeling of plug-in hybrid electric vehicles”, Applied Energy 2013; 103: 488-506.

[16] A. Biswas and A. Emadi, "Energy Management Systems for Electrified Powertrains: State-of-the-Art Review and Future Trends", IEEE Transactions on Vehicular Technology 2019; 68(7): 6453-6467.

[17] S. G. Wirasingha, A. Emadi, "Classification and Review of Control Strategies for Plug-In Hybrid Electric Vehicles", IEEE Transactions on Vehicular Technology 2011; 60(1): 111-22.

[18] F. Millo, L. Rolando, R. Fuso, F. Mallamo, “Real CO2 emissions benefits and end user’s operating costs of a plug-in Hybrid Electric Vehicle”, Applied Energy 2014; 114: 563-71.

[19] P.G. Anselma, G. Belingardi, A. Falai, C. Maino, F. Miretti, D. Misul et al., "Comparing Parallel Hybrid Electric Vehicle Powertrains for Real-world Driving," 2019 AEIT International Conference of Electrical and Electronic Technologies for Automotive (AEIT AUTOMOTIVE), Torino, Italy, 2019, pp. 1-6.

[20] S. Ebbesen, C. Donitz, L. Guzzella, "Particle swarm optimisation for hybrid electric drive-train sizing", Int. J. Vehicle Design, Vol. 58, Nos. 2/3/4, 2012.

[21] Paganelli, G., Guezennec, Y., and Rizzoni, G., "Optimizing Control Strategy for Hybrid Fuel Cell Vehicle," SAE Technical Paper 2002-01-0102, 2002.

[22] S. Delprat, T. Hofman, S. Paganelli, "Hybrid Vehicle Energy Management: Singular Optimal Control", IEEE Transactions on Vehicular Technology 2017; 66(11): 9654-66.

[23] N. Kim, S. Cha, H. Peng, "Optimal Control of Hybrid Electric Vehicles Based on Pontryagin's Minimum Principle", IEEE

Transactions on Control Systems Technology 2011; 19(5): 1279-87.
[24] Dabadie, J., Sciarretta, A., Font, G., and Le Berr, F., "Automatic Generation of Online Optimal Energy Management Strategies for Hybrid Powertrain Simulation," SAE Technical Paper 2017-24-0173, 2017.
[25] C. Hou, M. Ouyang, L. Xu, H. Wang, “Approximate Pontryagin’s minimum principle applied to the energy management of plug-in hybrid electric vehicles”, Applied Energy 2014; 115: 174-89.
[26] X. Zhang, H. Peng, J. Sun, “A near-optimal power management strategy for rapid component sizing of power split hybrid vehicles with multiple operating modes,” American Control Conference(ACC), 2013: 5972-77.
[27] Z. Qin, Y. Luo, W. Zhuang, Z. Pan, K. Li, H. Peng, “ Simultaneous optimization of topology, control and size for multi-mode hybrid tracked vehicles“, Applied Energy 2018; 212: 1627-41.
[28] P.G. Anselma, Y. Huo, J. Roeleveld, G. Belingardi, A. Emadi, “Slope-weighted Energy-based Rapid Control Analysis for Hybrid Electric Vehicles”, IEEE Transactions on Vehicular Technology 2019; 68(5): 4458 – 66.
[29] P.G. Anselma, Y. Huo, E. Amin, J. Roeleveld, A. Emadi, G. Belingardi, “Mode-shifting Minimization in a Power Management Strategy for Rapid Component Sizing of Multimode Power Split Hybrid Vehicles”, SAE Technical Paper 2018-01-1018, 2018.
[30] P.G. Anselma, Y. Huo, J. Roeleveld, A. Emadi, G. Belingardi, “Rapid optimal design of a multimode power split hybrid electric vehicle transmission”, Proc. IMechE Part D: J. Automobile Engineering 2019; 233(3): 740-62.
[31] X. Zhang, H. Peng, J. Sun, "A Near-Optimal Power Management Strategy for Rapid Component Sizing of Multimode Power Split Hybrid Vehicles", IEEE Transactions on Control Systems Technology 2015; 23(2): 609-18.
[32] L. Guzzella, A. Amstutz, "CAE tools for quasi-static modeling and optimization of hybrid powertrains", IEEE Transactions on Vehicular Technology 1999; 48(6): 1762-69.
[33] R.E. Bellman, E. Lee, “History and development of dynamic programming”, IEEE Control Systems Magazine 1984; 4(4): 24-28.
[34] J. Lempert, B. Vadala, K. Arshad-Aliy, J. Roeleveld and A. Emadi, "Practical Considerations for the Implementation of Dynamic Programming for HEV Powertrains," 2018 IEEE Transportation Electrification Conference and Expo (ITEC), Long Beach, CA, 2018, pp. 755-760.
[35] O. Sundstrom and L. Guzzella, "A generic dynamic programming Matlab function," 2009 IEEE Control Applications, (CCA) & Intelligent Control, (ISIC), St. Petersburg, 2009, pp. 1625-30.
[36] P.G. Anselma, G. Belingardi, "Next generation HEV powertrain design tools: roadmap and challenges," SAE Technical Paper 2019-01-2602, 2019.
[37] J. Liu, H. Peng, "A systematic design approach for two planetary gear split hybrid vehicles", Vehicle System Dynamics 2010; 48(11): 1395-412.
[38] A. Bayrak, Y. Ren, P. Papalambros, "Design of Hybrid-Electric Vehicle Architectures Using Auto-Generation of Feasible Driving Modes", Proceedings of the ASME 2013 International Design Engineering Technical Conferences and Computers and Information in Engineering Conference, Portland, OR, USA, 2013, pp. 1-9.
[39] W. Zhuang, X. Zhang, Y. Ding, L. Wang, X. Hu, “Comparison of multi-mode hybrid powertrains with multiple planetary gears,” Applied Energy 2016; 178(C):624-632.
[40] X. Zhang, S. Eben Li, H. Peng, J. Sun, "Efficient Exhaustive Search of Power-Split Hybrid Powertrains With Multiple Planetary Gears and Clutches." ASME. J. Dyn. Sys., Meas., Control. 2015; 137(12): 121006.
[41] Dabadie, J., Sciarretta, A., Font, G., and Le Berr, F., "Automatic Generation of Online Optimal Energy Management Strategies for Hybrid Powertrain Simulation," SAE Technical Paper 2017-24-0173, 2017.
[42] J. M. Tyrus, R. M. Long, M. Kramskaya, Y. Fertman and A. Emadi, "Hybrid electric sport utility vehicles", IEEE Transactions on Vehicular Technology 2004; 53(5): 1607-22.
[43] T. Hofman and C. H. Dai, "Energy efficiency analysis and comparison of transmission technologies for an electric vehicle," 2010 IEEE Vehicle Power and Propulsion Conference, Lille, 2010, pp. 1-6.
[44] Y. Yang, X. Hu, H. Pei, Z. Peng, “Comparison of power-split and parallel hybrid powertrain architectures with a single electric machine: Dynamic programming approach”, Applied Energy 2016; 168: 683-690.
[45] X. Zhou, D. Qin, J. Hu, “Multi-objective optimization design and performance evaluation for plug-in hybrid electric vehicle powertrains”, Applied Energy 2017; 208: 1608-25.